⌘ *Author's Choice*

THE JOURNAL OF BIOLOGICAL CHEMISTRY VOL. 287, NO. 29, pp. 24774–24783, July 13, 2012

A Novel Fluorescent Cell Membrane-permeable Caged Cyclic ADP-ribose Analogue*[S]

Received for publication, December 2, 2011, and in revised form, May 15, 2012 Published, JBC Papers in Press, June 1, 2012, DOI 10.1074/jbc.M111.329854

Pei-Lin Yu[‡§], Zhe-Hao Zhang[§], Bai-Xia Hao[§], Yong-Juan Zhao[§], Li-He Zhang[‡], Hon-Cheung Lee[§], Liangren Zhang[‡1], and Jianbo Yue[§2]

From the [‡]State Key Laboratory of Natural and Biomimetic Drugs, School of Pharmaceutical Sciences, Peking University, Beijing 100191 and the [§]Department of Physiology, the University of Hong Kong, Hong Kong, China

Background: The available agonists for cADPR, an endogenous Ca^{2+}-mobilizing nucleotide, are either weak or not cell-permeant.
Results: We synthesized a coumarin-caged isopropylidene-protected cIDPRE (Co-*i*-cIDPRE), which is a potent and cell-permeant cADPR agonist.
Conclusion: Uncaging of Co-*i*-cIDPRE activates RyRs for Ca^{2+} mobilization and triggers Ca^{2+} influx via TRPM2.
Significance: Co-*i*-cIDPRE should provide a valuable tool to study cADPR/Ca^{2+} signaling.

Cyclic adenosine diphosphate ribose is an endogenous Ca^{2+} mobilizer involved in diverse cellular processes. A cell membrane-permeable cyclic adenosine diphosphate ribose analogue, cyclic inosine diphosphoribose ether (cIDPRE), can induce Ca^{2+} increase in intact human Jurkat T-lymphocytes. Here we synthesized a coumarin-caged analogue of cIDPRE (Co-*i*-cIDPRE), aiming to have a precisely temporal and spatial control of bioactive cIDPRE release inside the cell using UV uncaging. We showed that Co-*i*-cIDPRE accumulated inside Jurkat cells quickly and efficiently. Uncaging of Co-*i*-cIDPRE evoked Ca^{2+} release from endoplasmic reticulum, with concomitant Ca^{2+} influx in Jurkat cells. Ca^{2+} release evoked by uncaged Co-*i*-cIDPRE was blocked by knockdown of ryanodine receptors (RyRs) 2 and 3 in Jurkat cells. The associated Ca^{2+} influx, on the other hand, was abolished by double knockdown of Stim1 and TRPM2 in Jurkat cells. Furthermore, Ca^{2+} release or influx evoked by uncaged Co-*i*-cIDPRE was recapitulated in HEK293 cells that overexpress RyRs or TRPM2, respectively, but not in wild-type cells lacking these channels. In summary, our results indicate that uncaging of Co-*i*-cIDPRE incites Ca^{2+} release from endoplasmic reticulum via RyRs and triggers Ca^{2+} influx via TRPM2.

Cyclic adenosine diphosphate ribose (cADPR)[3] is an endogenous second messenger that mobilizes Ca^{2+} release in a wide variety of cell types and species. cADPR is formed from nicotinamide adenine dinucleotide (NAD) by ADP-ribosyl cyclases. CD38 is the main mammalian ADP-ribosyl cyclase. cADPR elicits Ca^{2+} release from the endoplasmic reticulum (ER) through the ryanodine receptors (RyRs) and can also modulate the transient receptor potential cation channel subfamily M member 2 (TRPM2) for Ca^{2+} influx (1–4). Although all three RyR isoforms have been shown to mediate cADPR-induced Ca^{2+} release (1–3), evidence regarding whether cADPR acts directly on the receptors is lacking (5). Instead, two cADPR-binding proteins, 140- and 100-kDa proteins, have been identified in sea urchin egg homogenates by using 8-N_3-cADPR, a cADPR antagonist, as a photoaffinity probe (6). Also, both calmodulin and FK506-binding protein have been shown to be required for cADPR action (1–3, 7–9). These data suggest that cADPR does not directly bind to the ryanodine receptors, but acts through some intermediate proteins, whose definitive identities remain to be established.

Given the important physiological role of cADPR, a number of cADPR analogues have been generated chemically or from the corresponding NAD analogues using ADP-ribosyl cyclase (10–13). The first successful total chemical synthesis of cADPR and its analogues was not reported until 2000 by Shuto and co-workers (14) despite repeated attempts right after cADPR was discovered. In the Shuto method, a large group is introduced to the 8-position of purine to force the nucleoside to adopt the *syn* conformation, such that the subsequent intramolecular cyclization could be achieved. A later improvement, using an activated precursor, succeeded in intramolecular pyrophosphate formation even without a large substituent at the 8-position (14). The success of chemical synthesis has promoted the synthesis of a number of cADPR analogues that could not be synthesized by the enzymatic method in recent years (15–23). These analogues can be grouped into two categories: either derivatives of cyclic IDP-ribose (cIDPR) or cyclic

* This work was supported by Research Grant Council (RGC) Grants HKU 784710M, HKU 782709M, and HKU 785911M, a National Natural Science Foundation of China (NSFC)/RGC grant from Hong Kong (Grant N_HKU 737/09), NSFC Grant 20910094 and 90713005, and a Special Fellow Award from the Leukemia and Lymphoma Society of America (to J. Y.).
⌘ *Author's Choice*—Final version full access.
[S] This article contains supplemental Figs. S1–S8 and Table S1.
[1] To whom correspondence may be addressed. E-mail: liangren@bjmu.edu.cn.
[2] To whom correspondence may be addressed. E-mail: jyue@hku.hk.
[3] The abbreviations used are: cADPR, cyclic ADP-ribose; ADPR, ADP-ribose; cIDPR, cyclic IDP-ribose; cIDP-DE, N^1-[(phosphoryl-*O*-ethoxy)-methyl]-N^9-[(phosphoryl-*O*-ethoxy)-methyl]-hypoxanthine-cyclic pyrophosphate; cIDPRE, N^1-[(5″-*O*-phosphorylethoxy)methyl]-5′-*O*-phosphorylinosine 5′,5″-cyclic pyrophosphate; Co-*i*-cIDPRE, coumarin-caged isopropylidene-protected cIDPRE; cTDPRE, cyclic triazole diphosphoribose; NPE-cADPR, 1-(2-Nitrophenyl)ethyl caged cyclic ADP-ribose; TRPM2, transient receptor potential cation channel subfamily M member 2; SOC, store-operated channel; RyR, ryanodine receptor; ER, endoplasmic reticulum; HBSS, Hanks' balanced salt solution; 8-N_3-cADPR, 8-azido-cyclic ADP-ribose.

ADP-carbocyclic-ribose. These cADPR analogues have been used to elucidate some important structural and functional properties of cADPR (13).

Like all other cytosolic messengers, cADPR is hydrophilic and cannot cross the plasma membrane. Therefore, cell-permeant cADPR analogues are valuable research tools in dissecting the mechanism of cADPR-induced Ca^{2+} release. A number of cADPR analogues with modification at the N-1 position have been synthesized by us, such as those using an ether linkage to substitute for the ribose of cIDPR (16–23). These mimics not only retain the Ca^{2+}-releasing activity, but more importantly, are also membrane-permeant. A moderate agonistic analogue of cADPR is obtained after both northern and southern riboses are substituted with ether linkages (19). More recently, the nucleobase of cADPR has been simplified; a novel cADPR analogue, cTDPRE, has been synthesized using click chemistry, and it is biologically active in human Jurkat T cells (22, 24). However, the main drawback for these cADPR agonists is that they are not particularly potent. Here we synthesized a novel fluorescent caged cADPR analogue, coumarin-caged isopropylidene-protected cIDPRE (Co-*i*-cIDPRE), and found that it is a potent and controllable cell-permeant cADPR analogue. Moreover, we demonstrated that uncaging of Co-*i*-cIDPRE activates RyRs for Ca^{2+} mobilization and triggers Ca^{2+} influx via TRPM2.

EXPERIMENTAL PROCEDURES

Chemistry—All of the chemical reagents used were purchased from Sigma. Compound **1** was synthesized using the method described previously (25). Phosphorylation of compound **1** was then performed (26). Briefly, compound **1** (40 mg, 0.1 mmol) was dissolved in a solution of 1*H*-tetrazole (70 mg, 1 mmol) in CH_3CN (2 ml) with argon protection and was stirred for 15 min at room temperature. Next, dibenzyl *N*,*N*-diisopropylphosphoramidite (142 mg, 0.6 mmol) was added dropwise over 1 min. After stirring overnight, the reaction mixture was cooled to 0 °C, and *tert*-butyl hydroperoxide (0.18 ml of 5.5 M solution in decane) was added. After another 4 h of the reaction being exposed to air, this phosphorylation procedure was finished. Flash chromatography was then used to purify compound **2** (70 mg, 75% yield). Hereafter, compound **2** (50 mg, 0.055 mmol) was suspended with 10% Pd/C (20 mg) in CH_3OH (5 ml), and the suspension was stirred at room temperature under H_2 (0.4 atm) for 1 h for debenzylation. The catalyst was subsequently filtered off, and the filtrate was evaporated. The dried filtrate was dissolved in dry dimethyl sulfoxide (DMSO) with 1,1′-carbonyldiimidazole (45 mg, 0.28 mmol) and underwent a microwave cyclization at 85 °C for 1 h. Afterward, compound **3** (14.5 mg, 40% yield), as a triethylamine salt, was purified by HPLC on a C18 reversed phase column, eluting with a linear gradient of 0–60% CH_3CN in triethylammonium acetate buffer (0.05 M, pH 7.5). Compound **3** was subsequently changed to tetrabutylamine salt by base exchange reaction with 2 eq of tetra-*n*-butylammonium hydroxide. After lyophilization, compound **3** tetrabutylamine salt (12 mg) was dissolved in anhydrous CH_3CN (2 ml) and mixed with 4-(bromomethyl)-7-acetoxycoumarin (18 mg, 0.06 mmol). This mixture was allowed reflux under 85 °C for 5 h. Finally, the target compound **4** (3.3 mg, 30% yield) was purified by HPLC on a C18 reversed phase column, eluting with a linear gradient of 0–80% CH_3CN in triethylammonium acetate buffer (0.05 M, pH 7.5) (see Fig. 1). According to the ^1H NMR spectrum, this caged structure represented a mixture of more than one monocaged isomer (supplemental Fig. S1). They all could be efficiently photolysed into *i*-cIDPRE under the UV flash as detected by HPLC analysis (see Fig. 2*B*). ^1H NMR (500 MHz, D_2O) δ8.4, 8.1 (s, each 1 H), 8.0–6.0 (m, 4 H), 5.90 (m, 1 H), 5.28 (m, 1 H), 4.42 (m, 1 H), 4.1–3.4 (m, 11 H), 2.3–2.1 (m, 3 H, -$COCH_3$), 1.55, 1.38 (each s, each 3 H); all of the other peaks were subjected to the signals from tetrabutylamine salt. ^{31}P NMR (121 MHz, D_2O) δ-10.30, -10.56 ppm. High resolution mass spectrometry (electrospray ionization, positive) for $C_{29}H_{32}O_{16}P_2$, calculated 755.1361 $[M+1]^+$, found 755.1359 (supplemental Fig. S1).

Cell Culture—The human Jurkat T-lymphocytes and human embryonic kidney (HEK) 293 cells were obtained from ATCC (Manassas, VA). HEK293 cells that overexpress RyR2 or RyR3 were kindly provided by Dr. King-Ho Cheung (University of Hong Kong). Jurkat cells were normally cultured in RPMI medium 1640 (Invitrogen) supplemented with 10% fetal bovine serum (FBS), 100 units/ml penicillin/streptomycin, and 2 mM Hepes buffer (pH 7.4) at 5% CO_2 and 37 °C. HEK293 cells were cultured in DMEM medium (Invitrogen) supplemented with 10% FBS and 100 units/ml penicillin/streptomycin at 5% CO_2 and 37 °C.

Western Blot Analysis—Western blot analysis was performed as described previously (27). Briefly, cells were lysed in an ice-cold lysis buffer (50 mM HEPES at pH 7.5, 0.15 M NaCl, 1 mM EDTA, 1% Nonidet P-40, 150 μM PMSF, 10 mM NaF, 10 ng/ml leupeptin, 1 mM DTT, and 1 mM sodium vanadate) and passed through a 21-gauge needle several times to disperse any large aggregates. Protein concentrations of the cell lysates were determined by Bradford protein assay. 30 μg of protein/lane was diluted in the standard SDS-sample buffer and subjected to electrophoresis on 8 or 10% SDS-polyacrylamide gels. Proteins were then transferred to an Immobilon PVDF membrane (Millipore, Billerica, MA), blocked with 5% milk in TBST (20 mM Tris, 150 mM NaCl, pH 7.6), and incubated with the primary antibody (RyRs, SC-13942, Santa Cruz Biotechnology, 1:500 dilution; Stim1, 610954, BD Biosciences, 1:1000 dilution; TRPM2, SC-19198, Santa Cruz Biotechnology, 1:500 dilution) overnight. After washing with TBST, the blots were probed with a secondary antibody (1:3000 dilution) for detection by chemiluminescence.

Ryr2, Ryr3, TRPM2, and Stim1 shRNA Lentivirus Production and Infection—The optimal 21-mers were selected in the human *ryr2*, *ryr3*, *trmp2*, and *stim1* genes (supplemental Table S1). One 21-mer was selected in the *GFP* gene as a control. These sequences were then cloned into pLKO.1 vector for expressing shRNA. The shRNA lentivirus production was performed in 293T cells as described previously (28). For infection, Jurkat cells were plated at a density of 3×10^5 cells/well in 6-well plates. On the next day, 100 μl pools of shRNAs lentivirus were added to the cells in fresh medium containing 8 μg/ml Polybrene. Two days later, cells were selected in fresh medium containing puromycin (3 μg/ml) for 3–5 days. The puromycin-resistant cells were pooled, and the knockdown efficiency was

verified by both quantitative real-time RT-PCR and/or Western blot analyses. TRPM2 shRNA 1 was used for the double knockdown with Stim1.

Quantitative Real-time RT-PCR Analysis—The quantitative real-time RT-PCR using the iScript™ one-step kit with SYBR® Green (Invitrogen) was performed normally in Bio-Rad Mini-Opticon™ real-time PCR detection system according to the manufacturer's instructions. The primers for detecting *ryr2* or *ryr3* mRNAs are listed in supplemental Table S1.

Transient Transfection—HEK293 cells were plated at a density of 3×10^5 cells/well in 6-well plates. On the next day, 2 h before transfection, the medium was changed to an antibiotic-free medium. The pCI-CFP-hTRPM2 or empty vector pCI-CFP was then transfected into cells by Lipofectamine™ 2000 (Invitrogen). 24 h after transfection, the medium was changed to regular medium, and TRPM2-CFP- or CFP-positive cells were finally used for Ca^{2+} measurement after another 24 h.

Ca^{2+} Measurement—Ca^{2+} measurement was performed as described previously (29). Briefly, Jurkat cells (2×10^5 cells/well) or HEK293 cells (6×10^4 cells/well) were plated in 24-well plates coated with 100 or 10 μg/ml poly-L-lysine (Sigma, P6282), respectively. Both cells were incubated first in serum-free medium overnight for adherence before changing to regular medium. The adherent cells were incubated with 2 μM Fluo-4 AM (Invitrogen) in Hanks' balanced salt solution (HBSS) with or without calcium for 30 min in the dark at 37 °C. The cells were then washed with HBSS twice and incubated in 200 μl of HBSS. Thereafter, the cells were put on the stage of an Olympus inverted epifluorescence microscope and incubated with or without caged compound for 5 min followed by UV (370 nm) flash for 1 s, which was repeated every 7 s during the measurement of fluorescence intensity at 480 nm using a 20× objective. Images were collected by a CCD camera every 7 s and analyzed by the cell R imaging software. For Ca^{2+} mobilization in single cell, a 60× oil immersion objective was used.

Data Analysis—In each measurement, intracellular Ca^{2+} concentration was calculated using the formula, $[Ca^{2+}]_i = K_d(F - F_{min})/(F_{max} - F)$ (K_d = 345 nM), if the value fit within the indicating ranges for Fluo-4. F_{max} was determined by exposing cells to 10 mM Ca^{2+} and 5 μM ionomycin, and F_{min} was determined by the addition of 4 mM EGTA and 5 μM ionomycin to cells. For Ca^{2+} concentrations that went beyond the Fluo-4-indicating range, F/F_0 (F_0: fluorescence intensity at the start point of measurement) were used instead. All of the data were averaged from at least three independent experiments. Significant differences of peak Ca^{2+} level and rise time for maximum Ca^{2+} concentration between groups were determined by the Student's t test, in which $p < 0.05$ was validated to be significant.

Permeability Kinetics—Jurkat cells were plated in 24-well plates as described above. The cells were then incubated with 200 μM Co-*i*-cIDPRE for up to 5 min. Thereafter, cells were washed with regular HBSS medium and incubated in medium without Co-*i*-cIDPRE for another 25 min. At the indicated time points, cells at three individual wells were washed again with HBSS and subjected to a reading of the fluorescence intensity at 337 nm.

RESULTS

Design and Synthesis of a New Caged Isopropylidene-protected cADPR Analogue, Co-i-cIDPRE—Many derivatives of cADPR have been synthesized enzymatically or chemically (13). Some of these cADPR mimics are strong cADPR agonists, but like cADPR itself, are cell-impermeant, such as 3-deaza-cADPR (30). Others are cell-permeant, but are weak agonists of cADPR, such as cIDP-DE and cIDPRE (18, 19). In addition, almost all of these cADPR agonists are difficult to synthesize, and some of them are unstable. Among them, cIDPRE is a relatively stable and permeable analogue of cADPR, and we have been able to simplify the synthesis route of cIDPRE from the original eight steps (25) to five steps with good yield (Fig. 1*A*). Two important improvements were used. Firstly, dibenzyl *N*,*N*-diisopropylphosphoramidite was used in the phosphorylation step, which allowed us to carry out intramolecular cyclization right after debenzylation by hydrogenation without further HPLC purification. Secondly, intramolecular cyclization was achieved by 1,1′-carbonyldiimidazole catalysis under a microwave condition, which allowed using high concentration of reagents and resulted in a shorter reaction time and higher yield. In the process of simplifying the synthesis of cIDPRE, we found that the isopropylidene-protected cIDPRE (*i*-cIDPRE) was more stable than cIDPRE. In addition, *i*-cIDPRE evoked a Ca^{2+} increase in Jurkat cells at a similar potency as cIDPRE (supplemental Fig. S2).

To improve the biological activity of *i*-cIDPRE, we reasoned that adding a caged group to one of the phosphates on *i*-cIDPRE could increase its membrane permeability and enable it to accumulate inside cells without mobilizing Ca^{2+}. Photolysis by UV can then release the bioactive cIDPRE, providing more precise control of its Ca^{2+}-signaling function. We chose coumarin as the caged group not only because of its lipophilicity, which can enhance membrane permeability, but also because it is fluorescent, which can facilitate the monitoring of its permeability kinetics. To further increase lipid solubility and stability of the caged compound (31), the 7-OH on the coumarin was acetylated. The synthesis of the Co-*i*-cIDPRE is shown in Fig. 1*B*. Characterizations of the compound using ^{1}H NMR, ^{31}P NMR, and high resolution mass spectrometry are consistent with the predicted structure (supplemental Fig. S1). It is also noted that the final Co-*i*-cIDPRE fraction collected during HPLC purification contains a mixture of isomers that were caged at different phosphates of *i*-cIDPRE and/or with different conformations, although only one caged group existed in it.

We found that Co-*i*-cIDPRE was relatively stable, with only 17.6% hydrolyzed to *i*-cIDPRE after storage in its lyophilized form at −20 °C in the dark for 240 days (data not shown). The fluorescence spectrum of Co-*i*-cIDPRE is shown in Fig. 2*A*, with an excitation maximum at 337 nm and an emission maximum at 475 nm. After continuous UV illumination for 10 min, Co-*i*-cIDPRE was almost completely photolysed into bioactive *i*-cIDPRE and coumarin (Fig. 2*B*). The permeation and efflux kinetics of Co-*i*-cIDPRE in Jurkat cell was also analyzed. As shown in Fig. 2*C*, the fluorescent Co-*i*-cIDPRE accumulated inside Jurkat cells quickly within 3 min of incubation and reached saturation within 5 min. After Co-*i*-cIDPRE was

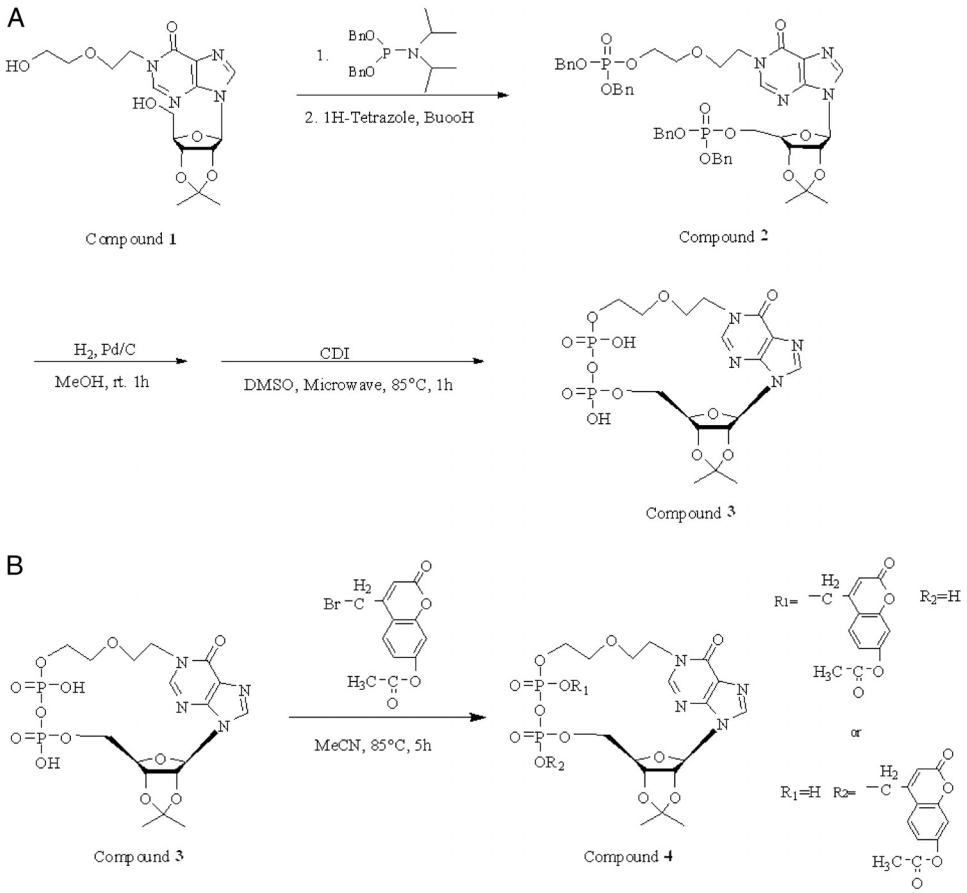

FIGURE 1. **Synthesis route of Co-*i*-cIDPRE.** *A*, synthesis of *i*-cIDPRE. *B*, synthesis of Co-*i*-cIDPRE.

removed from the medium at 5 min, the fluorescent intensity of the cells was only slowly decreased over time, indicating that the efflux rate of Co-*i*-cIDPRE is small. The image of Jurkat cells loaded with the fluorescent Co-*i*-cIDPRE is shown in Fig. 2*D*, and the quantitative analysis of the influx and efflux of Co-*i*-cIDPRE is shown in supplemental Fig. S3.

Pharmacological Characterization of Co-i-cIDPRE—Although Co-*i*-cIDPRE is fluorescent, no interference was observed when using either Fluo-4 or Fluo-3 to monitor its Ca^{2+}-mobilizing property. As expected, without UV uncaging, Co-*i*-cIDPRE did not evoke any Ca^{2+} changes in Jurkat cells. Subsequent UV flashes evoked Ca^{2+} increases that were much higher than that induced by either cIDPRE itself or by photolysing another caged analogue of cADPR, NPE-cADPR, at the same concentration (Fig. 3*A* and supplemental Fig. S4). Controls showed that in cells without the Ca^{2+} indicator, uncaging of Co-*i*-cIDPRE did not produce any fluorescence changes, indicating that the signals indeed reflected Ca^{2+} changes (data not shown). Removal of external Co-*i*-cIDPRE by washing cells with regular HBSS buffer altered neither the rise time nor the amplitude of the Ca^{2+} increases, indicating that it was the photolysed cIDPRE inside the cells that was responsible for inducing the Ca^{2+} changes (Fig. 3*B*). The extent of the photolysis-induced Ca^{2+} changes was dependent on the concentration of Co-*i*-cIDPRE in both the presence and the absence of extracellular Ca^{2+}, although the Ca^{2+} increases observed in the presence of extracellular Ca^{2+} were much higher and sustained, indicating that Ca^{2+} influx also contributed (Fig. 3, *C* and *D*, and supplemental Fig. S5). Pretreating cells with thapsigargin, a specific sarco/endoplasmic reticulum Ca^{2+}-ATPase (SERCA) inhibitor, abolished the Ca^{2+} increase in the absence of external Ca^{2+}, consistent with the fact that cADPR induces Ca^{2+} release from the ER pools (Fig. 3*E*). In summary, these data demonstrate that UV uncaging of Co-*i*-cIDPRE induces Ca^{2+} release from ER pools, accompanied with extracellular Ca^{2+} influx.

Requirement of RyRs for Uncaged Co-i-cIDPRE-induced Ca^{2+} Release—Ample evidence indicates that cADPR targets the ryanodine receptor on the ER membrane in many cell types (32, 33). Indeed, pretreatment with the RyR antagonist, high concentrations of ryanodine, significantly inhibited the Ca^{2+} increases triggered by uncaging the Co-*i*-cIDPRE in the Jurkat cells, in both the presence (Fig. 4*A*) and the absence (Fig. 4*B*) of extracellular Ca^{2+}. Both RyR2 and RyR3 were detected in the Jurkat cells. Thus, single or double knockdown experiments of both types of RyRs in Jurkat cells were performed (Fig. 4, *C* and *D*, and supplemental Fig. S6). Consistently, the ability of Co-*i*-cIDPRE to initiate Ca^{2+} release after UV flashes was significantly inhibited in these RyRs knockdown cells (Fig. 4*E*). Further support came from using another cell type, HEK293, which stably overexpresses either RyR2 or RyR3. Both cells were shown to be responsive to caffeine (supplemental Fig. S7) or photo-uncaging of Co-*i*-cIDPRE (Fig. 4*F*), whereas the wild-type HEK293 cells lacking the RyRs were nonresponsive to either treatment (Fig. 4*F* and supplemental Fig. S7). In sum-

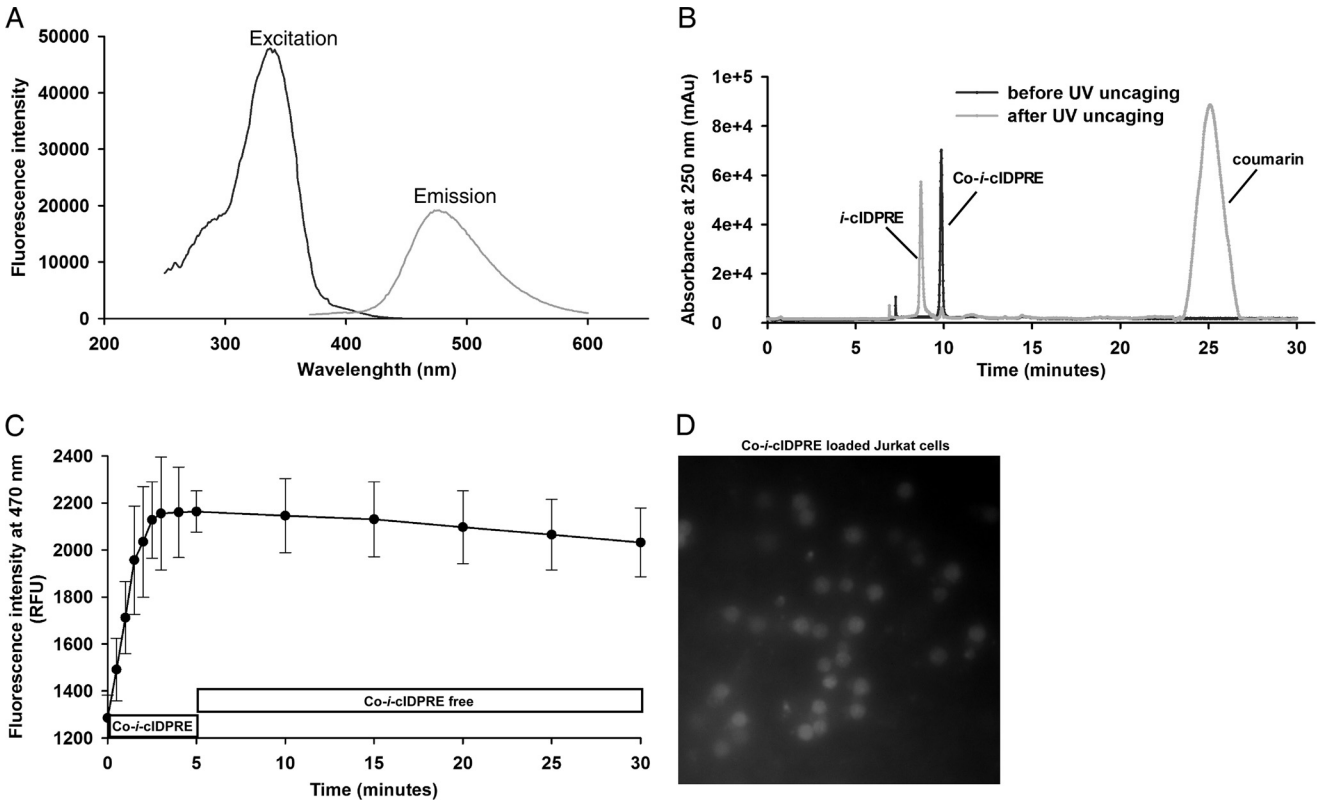

FIGURE 2. **Physical Characteristics of Co-*i*-cIDPRE.** *A*, fluorescence spectra of Co-*i*-cIDPRE with λ_{ex} = 337 nm and λ_{em} = 475 nm. *B*, HPLC analysis of Co-*i*-cIDPRE before and after UV photolysis. *C*, the permeation and efflux kinetics of Co-*i*-cIDPRE in human Jurkat cells. Cells were incubated with Co-*i*-cIDPRE (200 μM) in HBSS for 5 min; thereafter, Co-*i*-cIDPRE was washed away, and the cells were incubated in Co-*i*-cIDPRE-free HBSS for another 25 min. *RFU*, relative fluorescence units. *Error bars* indicate mean ± S.E. *D*, fluorescent image of Jurkat cells loaded with Co-*i*-cIDPRE (200 μM) (20×).

mary, our results definitely demonstrate that photolysis of Co-*i*-cIDPRE evokes Ca^{2+} release via RyRs.

Requirement of TRPM2 for Uncaged Co-i-cIDPRE-triggered Ca^{2+} Influx—It is conceivable that Ca^{2+} release from ER induced by uncaged Co-*i*-cIDPRE leads to partially depleted ER Ca^{2+} pools, which then activates canonical store-operated Ca^{2+} channels (SOCs) for Ca^{2+} influx. To confirm that canonical SOCs are responsible for the sustained phase of the Ca^{2+} increase induced by uncaged Co-*i*-cIDPRE, Stim1 was knocked down in Jurkat cells by shRNAs (supplemental Table S1 and Fig. 5*A*). The ability of uncaged cIDPRE-induced Ca^{2+} influx was markedly inhibited, but not abolished, in Stim1 knockdown cells (Fig. 5*D*). Because high concentrations of ryanodine or double knockdown of RyR2 and RyR3 also failed to completely block uncaged Co-*i*-cIDPRE-induced Ca^{2+} entry (Fig. 4, *A* and *E*), we suspected that other Ca^{2+} channels are also involved. Given that cADPR can modulate TRPM2 for Ca^{2+} influx (4, 34), we examined whether TRPM2 also contributes to uncaged Co-*i*-cIDPRE-induced Ca^{2+} influx. The expression of TRPM2 in Jurkat cells was effectively knocked down by a series of shRNAs (supplemental Table S1 and Fig. 5*B*). As shown in Fig. 5*D*, in TRPM2 knockdown cells, the sustained phase of the Ca^{2+} increase induced by photolysing Co-*i*-cIDPRE was also markedly inhibited, but not eliminated. Thus, both Stim1 and TRPM2 were knocked down in Jurkat cells (Fig. 5*C*), and Co-*i*-cIDPRE-induced Ca^{2+} influx was almost completely blocked in the double knockdown cells (Fig. 5*D*), in which the pattern of Ca^{2+} changes now resembled that observed in the absence of extracellular Ca^{2+} (Fig. 3*D*). These data indicated that both canonical SOCs and TRPM2 contribute to uncaged cIDPRE-induced Ca^{2+} influx in Jurkat cells. To further assess whether uncaged Co-*i*-cIDPRE directly activates TRPM2 for Ca^{2+} influx, a CFP-tagged TRPM2 was transiently expressed in HEK293 cells that lack endogenous TRPM2 channel (Fig. 6*A*). As shown in Fig. 6*B*, uncaging of Co-*i*-cIDPRE triggered Ca^{2+} influx only in TRPM2-CFP expressed HEK293 cells, but not in wild-type HEK293 cells lacking the TRPM2 channels. Similar results have been observed in NPE-cADPR-treated cells (Fig. 6*C*). Thus, these data clearly demonstrated that uncaging of Co-*i*-cIDPRE or NPE-cADPR directly activates TRPM2 for Ca^{2+} influx.

DISCUSSION

In this study, we describe the synthesis and characterization of a fluorescent caged analogue of cADPR, Co-*i*-cIDPRE. We found that Co-*i*-cIDPRE entered intact human Jurkat T-lymphocytes quickly and accumulated inside cells with small leakage. After UV photolysis, Co-*i*-cIDPRE induced a much stronger Ca^{2+} increase than that of cIDPRE itself or NPE-cADPR, the caged cADPR previously synthesized (35). The sources of the Ca^{2+} increase are from the ER Ca^{2+} pools, with concomitant Ca^{2+} influx. The antagonists for RyRs or knockdown of the RyRs in Jurkat cells eliminated uncaged Co-*i*-cIDPRE-evoked Ca^{2+} release, whereas knockdown of Stim1 and TRPM2 abolished the concomitant Ca^{2+} influx. Consistently, in another cell type, HEK293, uncaging

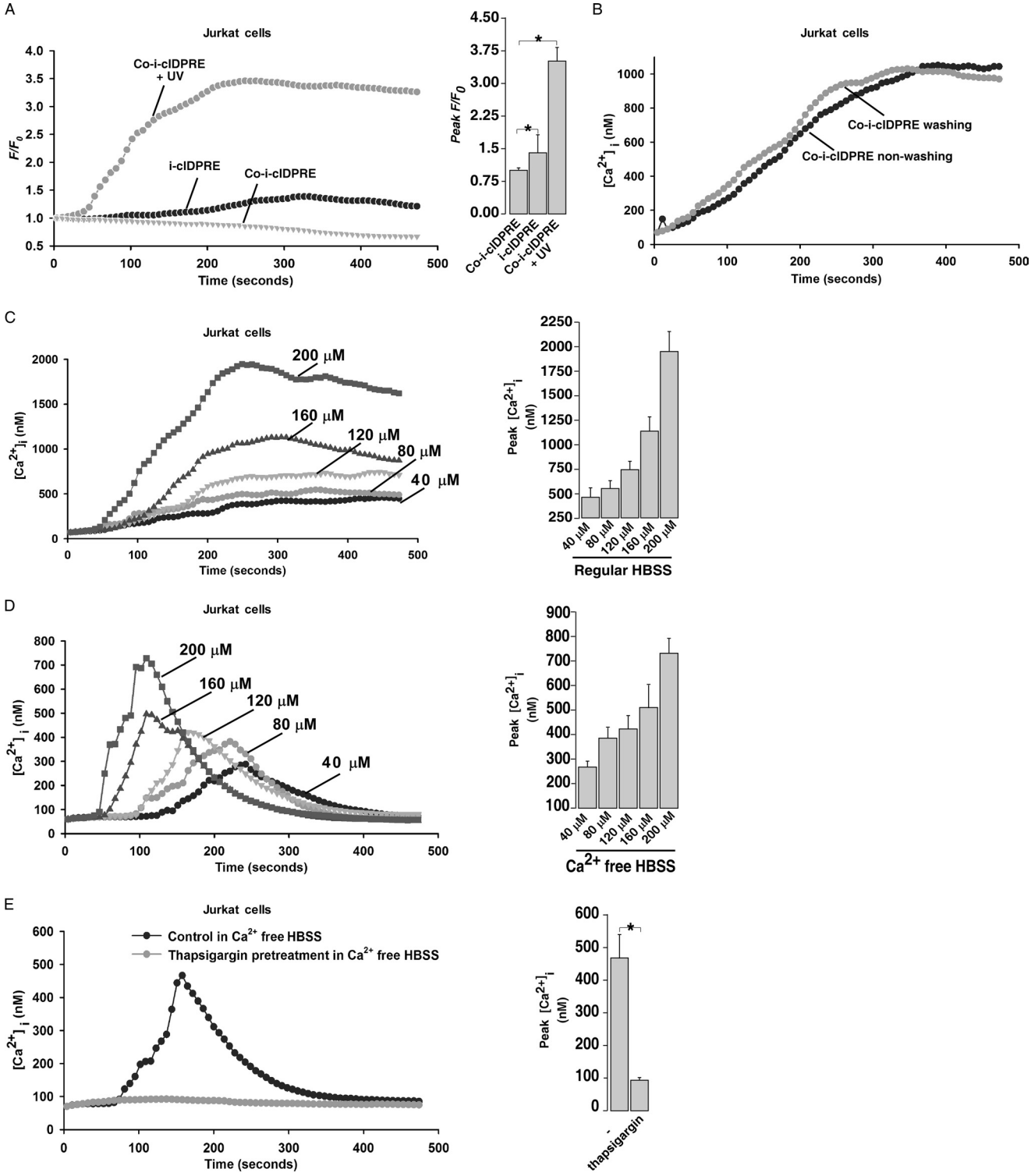

FIGURE 3. **Co-*i*-cIDPRE evokes Ca^{2+} increase in human Jurkat cells after UV photolysis.** *A*, Co-*i*-cIDPRE (200 μM) incited much stronger Ca^{2+} increases after UV photolysis than that by cIDPRE (200 μM) in Jurkat cells. Fluo-4-loaded Cells were incubated in regular HBSS containing extracellular Ca^{2+} during the experiment. *B*, after Fluo-4-loaded Jurkat cells were incubated with Co-*i*-cIDPRE (120 μM) in regular HBSS containing extracellular Ca^{2+}, washing away Co-*i*-cIDPRE in the medium did not have any effect on Ca^{2+} changes triggered by uncaging of Co-*i*-cIDPRE. *C* and *D*, in Fluo-4-loaded Jurkat cells, uncaging of Co-*i*-cIDPRE triggered Ca^{2+} increases in a dose-dependent manner in both the presence (*C*) and the absence of extracellular Ca^{2+} (*D*). *E*, in Fluo-4-loaded Jurkat cells, thapsigargin (10 μM) pretreatment abolished Co-*i*-cIDPRE (120 μM)-induced Ca^{2+} increases in the absence of extracellular Ca^{2+}. Data quantifications of $[Ca^{2+}]_i$ peak induced by drug treatment in *A*, *C*, *D*, and *E* were expressed as mean ± S.E., $n = 30-40$ cells, *, $p < 0.05$. In *A*, *C*, *D*, and *E*, cells were all continuously incubated with Co-*i*-cIDPRE throughout the experiments.

of Co-*i*-cIDPRE only induced Ca^{2+} release or triggered Ca^{2+} influx in cells that overexpress RyRs or TRPM2, respectively, but not in wild-type cells lacking these channels. Therefore, Co-*i*-cIDPRE is a cell-permeant cADPR analogue that can mobilize Ca^{2+} release via RyRs and induce Ca^{2+} influx via TRPM2 and SOCs.

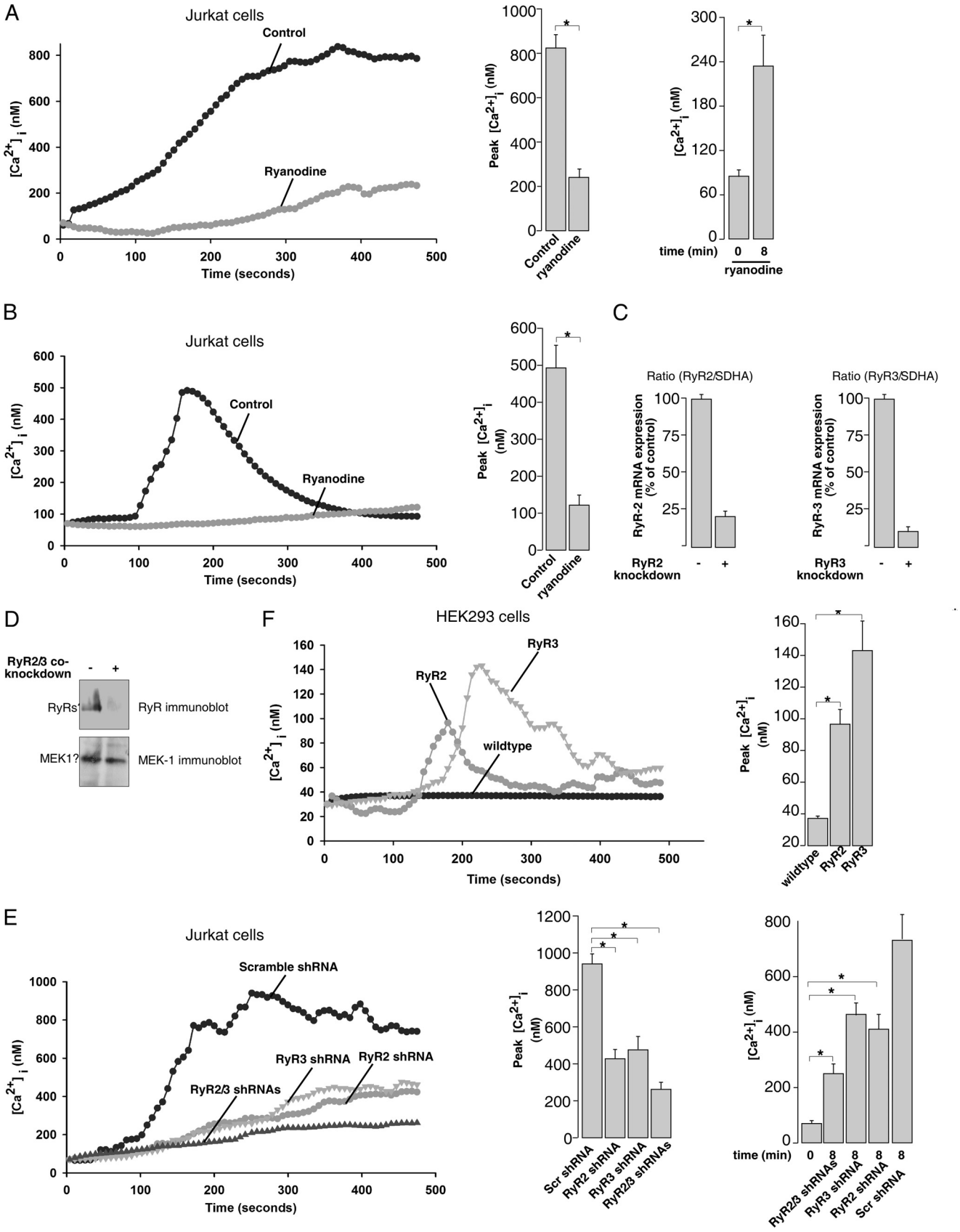
A
Jurkat cells
Control
Ryanodine
[Ca2+]i (nM)
Time (seconds)
Peak [Ca2+]i (nM)
Control
ryanodine
[Ca2+]i (nM)
time (min) 0 8
ryanodine
B
Jurkat cells
Control
Ryanodine
[Ca2+]i (nM)
Time (seconds)
Peak [Ca2+]i (nM)
Control
ryanodine
C
Ratio (RyR2/SDHA)
RyR-2 mRNA expression (% of control)
RyR2 knockdown - +
Ratio (RyR3/SDHA)
RyR-3 mRNA expression (% of control)
RyR3 knockdown - +
D
RyR2/3 co-knockdown - +
RyRs
RyR immunoblot
MEK1?
MEK-1 immunoblot
F
HEK293 cells
RyR3
RyR2
wildtype
[Ca2+]i (nM)
Time (seconds)
Peak [Ca2+]i (nM)
wildtype
RyR2
RyR3
E
Jurkat cells
Scramble shRNA
RyR3 shRNA
RyR2 shRNA
RyR2/3 shRNAs
[Ca2+]i (nM)
Time (seconds)
Peak [Ca2+]i (nM)
Scr shRNA
RyR2 shRNA
RyR3 shRNA
RyR2/3 shRNAs
[Ca2+]i (nM)
time (min) 0 8 8 8 8
RyR2/3 shRNAs
RyR3 shRNA
RyR2 shRNA
Scr shRNA

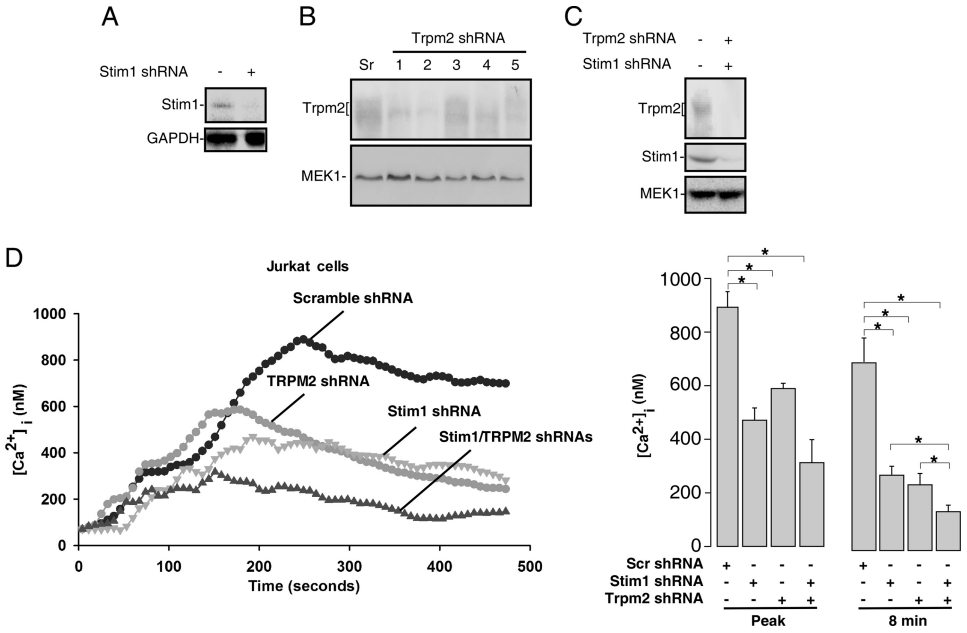

FIGURE 5. **The requirement of SOCs and TRPM2 for Co-*i*-cIDPRE-triggered Ca^{2+} influx in human Jurkat cells.** *A–C*, knockdown of Stim1 (*A*), TRPM2 (*B*), and both Stim1 and TRPM2 (*C*) in human Jurkat cells was verified by Western blot analysis with an antibody against Stim1 or TRPM2. *Sr lane* indicates scrambled shRNA. *D*, knockdown of Stim1, TRPM2, or both Stim1 and TRPM2 in Jurkat cells inhibited Co-*i*-cIDPRE-induced Ca^{2+} influx in Fluo-4-loaded cells after UV uncaging. Cells were all continuously incubated with Co-*i*-cIDPRE (120 μM) in regular HBSS containing extracellular Ca^{2+} throughout the experiments. Data quantifications of $[Ca^{2+}]_i$ peak or $[Ca^{2+}]_i$ at 8 min induced by uncaged Co-*i*-cIDPRE were expressed as mean ± S.E., $n = 30–40$ cells, *, $p < 0.05$. *Scr shRNA*, scrambled shRNA.

The parent compound of Co-*i*-cIDPRE, cIDPRE, has only moderate cell membrane permeability, and its synthesis is quite difficult (18). We simplified the synthesis of cIDPRE by using dibenzyl *N*,*N*-diisopropylphosphoramidite for diphosphorylation and performing cyclization under microwave-assisted conditions, which resulted in shorter steps and greater increase in yield. Adding a coumarin-caged group to one of the phosphates in *i*-cIDPRE and acetylation of the 7-OH on the coumarin further increase the liposolubility and stability of the caged compound, thereby facilitating its entry into cells (Fig. 2*C*). During the coumarin-caging step, isopropylidene protection on the two active hydroxyl groups in cIDPRE also greatly increased the yield of the caged compound (data not shown). Moreover, we found that the removal of Co-*i*-cIDPRE in the medium after cell loading had no effects on the Ca^{2+} increases induced by subsequent uncaging of Co-*i*-cIDPRE (Fig. 3*B*). These data not only demonstrate that it is the cytosolic, not extracellular, uncaged Co-*i*-cIDPRE that induces Ca^{2+} increases, but also are in line with the fact that Co-*i*-cIDPRE can accumulate inside cells with little of the caged compound leaking out (Fig. 2*D*). We reason that the acetylated group on the coumarin-caged compound is hydrolyzed by an esterase once it enters the cells, thereby decreasing the ability of the caged compound to leak out of the cells. Interestingly, we found that NPE-cADPR can also enter slowly into intact Jurkat cells and incite Ca^{2+} increases after UV photolysis. However, washing out the extra NPE-cADPR in the medium could markedly inhibit the ability of NPE-cADPR to induce Ca^{2+} increases, in both the rising time and the amplitude of Ca^{2+} current (supplemental Fig. S8). Thus, these data suggest that NPE-cADPR enters or exits the cell membrane via concentration gradients and can be removed by washing. Taken together, our data clearly demonstrated that Co-*i*-cIDPRE has the advantages of being a stable, highly cell-permeant, and potent cADPR analogue.

It has been shown that cADPR targets the RyR, but which specific isoform it targets remains to be determined (1–3). Here we showed that both RyR2 and RyR3 are expressed in Jurkat cells. Individual knockdown of these isoforms inhibited cIDPRE- or cADPR-induced Ca^{2+} release to a similar extent, whereas double knockdown of both isoforms abolished cADPR-induced Ca^{2+} release in Jurkat cells (Fig. 4*E*). These data indicate that cADPR does not distinguish either isoform. However, it still remains to be determined whether cADPR binds directly to the RyRs or through some unknown proteins. Recently, the long sought after store-operated Ca^{2+} entry proteins were identified using a genome-wide RNAi screen by several groups (36–38). Co-*i*-cIDPRE could be a valuable tool to be used in a similar cell based screening for cADPR-interacting proteins or regulators.

FIGURE 4. **The requirement of RyRs for Co-*i*-cIDPRE-triggered Ca^{2+} releases.** *A* and *B*, pretreatment of Fluo-4-loaded Jurkat cells with ryanodine (100 μM) inhibited Co-*i*-cIDPRE (120 μM)-induced Ca^{2+} increases in both the presence (*A*) and the absence (*B*) of extracellular Ca^{2+} after UV uncaging. *C*, knockdown of RyR2 or RyR3 in Jurkat cells was verified by real-time RT PCR analysis. *D*, double knockdown of RyR2 and RyR3 in Jurkat cells was confirmed by Western blot analysis with a pan-RyR antibody. *E*, knockdown of RyR2, RyR3, or both RyR2 and RyR3 inhibited Co-*i*-cIDPRE (120 μM)-induced Ca^{2+} increases in Jurkat cells after UV uncaging. Fluo-4-loaded cells were incubated in regular HBSS containing extracellular Ca^{2+} during the experiment. *F*, uncaging of Co-*i*-cIDPRE (120 μM) induced Ca^{2+} release only in HEK293 cells that stably express RyR2 or RyR3. HEK293 cells were loaded with Fluo-4 and incubated in regular HBSS containing extracellular Ca^{2+} during the experiments. Data quantifications of $[Ca^{2+}]_i$ peak or $[Ca^{2+}]_i$ at 8 min induced by uncaged Co-*i*-cIDPRE in *A*, *B*, *E*, and *F* were expressed as mean ± S.E., $n = 30–40$ cells, *, $p < 0.05$. In *A*, *B*, and *F*, cells were all continuously incubated with Co-*i*-cIDPRE throughout the experiments.

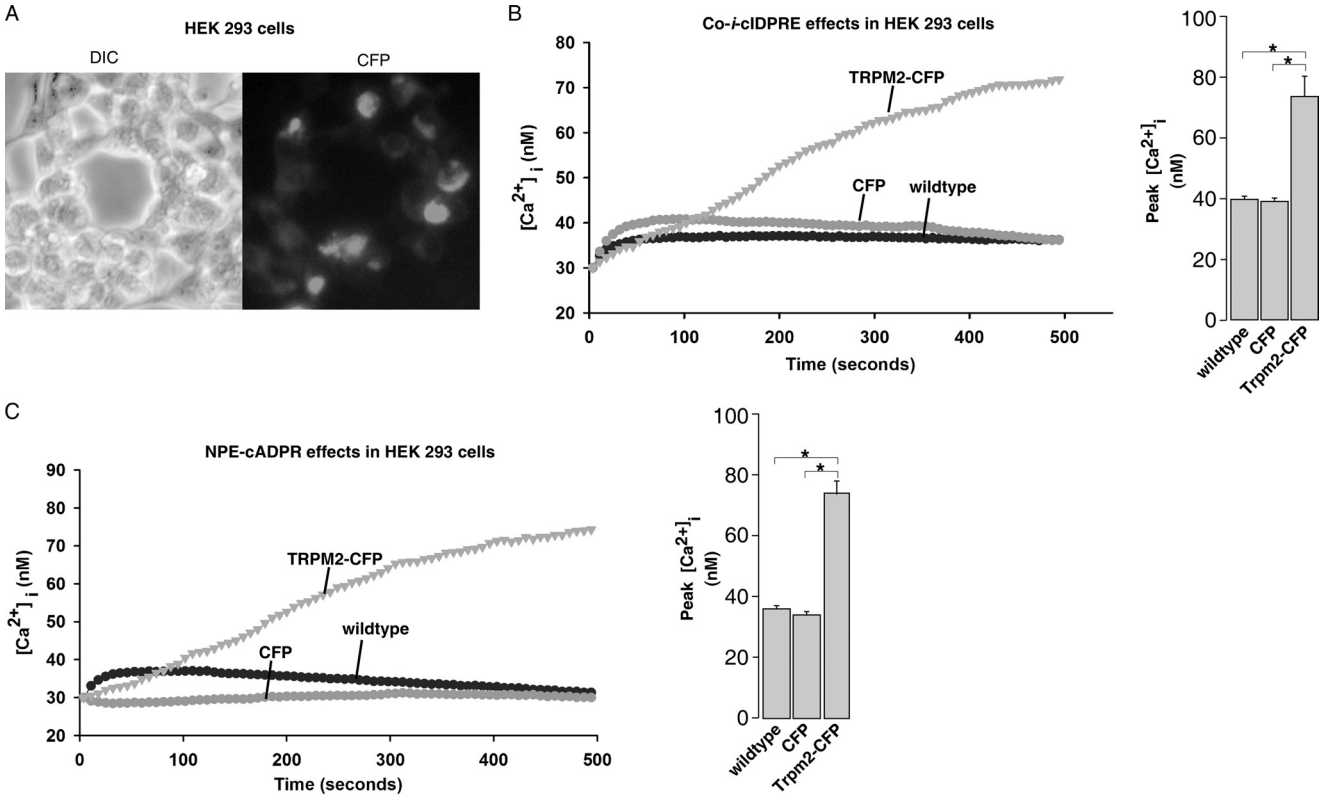

FIGURE 6. **Ca^{2+} influx triggered by Co-*i*-cIDPRE or NPE-cADPR in TRPM2-CFP-expressing HEK293 cells.** *A*, the differential interference contrast (*DIC*) and fluorescence images of HEK293 cells that transiently express TRPM2-CFP. *B* and *C*, uncaging of Co-*i*-cIDPRE (*B*) or NPE-cADPR (*C*) only induced Ca^{2+} influx in Fluo-4-loaded HEK293 cells that expresses TRPM2-CFP. Data quantifications of $[Ca^{2+}]_i$ peak induced by uncaged Co-*i*-cIDPRE were expressed as mean ± S.E., $n = 20–30$ cells, *, $p < 0.05$. Cells were all continuously incubated with Co-*i*-cIDPRE (120 μM) or NPE-cADPR (120 μM) in regular HBSS containing extracellular Ca^{2+} throughout the experiments.

TRPM2 is a Ca^{2+}-permeable, nonselective cation channel with a unique C-terminal diphosphoribose hydrolase and Nudix-like domain. The main activator for TRPM2 is intracellular ADP-ribose (ADPR) via its C terminus Nudix-like domain. TRPM2 can also be positively regulated by $[Ca^{2+}]_i$, cADPR, H_2O_2, and nicotinic acid adenine dinucleotide phosphate and negatively regulated by AMP and acidic pH. The mechanism for the regulation of TRPM2 by these factors, including cADPR, is not clear (34, 39, 40). It is generally thought that cADPR can act with ADPR to synergistically activate TRPM2 (34). It has also been proposed that the activating effect of cADPR may be due to its enzymatic conversion to ADPR inside cells, possibly via CD38 (41). Here we found that uncaging either Co-*i*-cIDPRE (Figs. 5*D* and 6*B*) or NPE-cADPR (Fig. 6*C* and data not shown) not only activated endogenous TRPM2 in Jurkat cells but also the exogenous expressed TRPM2 in HEK293 cells, producing Ca^{2+} influx in both cases. Photolysis of Co-*i*-cIDPRE generates only cIDPRE and coumarin (Fig. 2*B*), not ADPR. Likewise, photolysis of NPE-cADPR produces only cADPR, not ADPR (data not shown). Moreover, CD38 is not expressed in HEK293 cells (data not shown); thus, it is less likely that cADPR is converted to ADPR by CD38 in HEK293 cells. In addition, cIDPRE was found to be resistant to the hydrolytic activity of CD38 *in vitro* (17). Taken together, all these data support that cADPR directly activates TRPM2 for Ca^{2+} influx. However, the exact mechanism of how cADPR activates the TRPM2 channel remains to be determined.

Acknowledgments—We thank Richard Graeff and other members of the Yue laboratory for advice on the manuscript.

REFERENCES

1. Lee, H. C. (2001) Physiological functions of cyclic ADP-ribose and NAADP as calcium messengers. *Annu. Rev. Pharmacol. Toxicol.* **41,** 317–345
2. Guse, A. H. (2004) Biochemistry, biology, and pharmacology of cyclic adenosine diphosphoribose (cADPR). *Curr. Med. Chem.* **11,** 847–855
3. Galione, A., and Churchill, G. C. (2000) Cyclic ADP-ribose as a calcium-mobilizing messenger. *Sci. STKE* **2000,** PE1
4. Togashi, K., Hara, Y., Tominaga, T., Higashi, T., Konishi, Y., Mori, Y., and Tominaga, M. (2006) TRPM2 activation by cyclic ADP-ribose at body temperature is involved in insulin secretion. *EMBO J.* **25,** 1804–1815
5. Thomas, J. M., Masgrau, R., Churchill, G. C., and Galione, A. (2001) Pharmacological characterization of the putative cADP-ribose receptor. *Biochem. J.* **359,** 451–457
6. Walseth, T. F., Aarhus, R., Kerr, J. A., and Lee, H. C. (1993) Identification of cyclic ADP-ribose-binding proteins by photoaffinity labeling. *J. Biol. Chem.* **268,** 26686–26691
7. Noguchi, N., Takasawa, S., Nata, K., Tohgo, A., Kato, I., Ikehata, F., Yonekura, H., and Okamoto, H. (1997) Cyclic ADP-ribose binds to FK506-binding protein 12.6 to release Ca^{2+} from islet microsomes. *J. Biol. Chem.* **272,** 3133–3136
8. Zhang, X., Tallini, Y. N., Chen, Z., Gan, L., Wei, B., Doran, R., Miao, L., Xin, H. B., Kotlikoff, M. I., and Ji, G. (2009) Dissociation of FKBP12.6 from ryanodine receptor type 2 is regulated by cyclic ADP-ribose but not β-adrenergic stimulation in mouse cardiomyocytes. *Cardiovasc. Res.* **84,** 253–262

9. Thomas, J. M., Summerhill, R. J., Fruen, B. R., Churchill, G. C., and Galione, A. (2002) Calmodulin dissociation mediates desensitization of the cADPR-induced Ca^{2+} release mechanism. *Curr. Biol.* **12,** 2018–2022
10. Shirato, M., Shuto, S., Ueno, Y., and Matsuda, A. (1995) Synthetic study on carbocyclic analogues of cyclic ADP-ribose. *Nucleic Acids Symp. Ser.* (*Oxf.*) 165–166
11. Shuto, S., and Matsuda, A. (2004) Chemistry of cyclic ADP-ribose and its analogues. *Curr. Med. Chem.* **11,** 827–845
12. Shuto, S. (2007) Design, synthesis, and biological activity of carbocyclic analogues of cyclic ADP-ribose, a Ca^{2+}-mobilizing second messenger. *Nucleic Acids Symp. Ser.* (*Oxf.*) 109–110
13. Morgan, A. J., and Galione, A. (2008) Investigating cADPR and NAADP in intact and broken cell preparations. *Methods* **46,** 194–203
14. Fukuoka, M., Shuto, S., Minakawa, N., Ueno, Y., and Matsuda, A. (2000) An efficient synthesis of cyclic IDP- and cyclic 8-bromo-IDP-carbocyclic-riboses using a modified Hata condensation method to form an intramolecular pyrophosphate linkage as a key step: an entry to a general method for the chemical synthesis of cyclic ADP-ribose analogues *J. Org. Chem.* **65,** 5238–5248
15. Zhang, B., Bailey, V. C., and Potter, B. V. (2008) Chemoenzymatic synthesis of 7-deaza cyclic adenosine 5′-diphosphate ribose analogues, membrane-permeant modulators of intracellular calcium release. *J. Org. Chem.* **73,** 1693–1703
16. Zhang, B., Wagner, G. K., Weber, K., Garnham, C., Morgan, A. J., Galione, A., Guse, A. H., and Potter, B. V. (2008) 2′-Deoxy cyclic adenosine 5′-diphosphate ribose derivatives: importance of the 2′-hydroxyl motif for the antagonistic activity of 8-substituted cADPR derivatives. *J. Med. Chem.* **51,** 1623–1636
17. Kirchberger, T., Wagner, G., Xu, J., Cordiglieri, C., Wang, P., Gasser, A., Fliegert, R., Bruhn, S., Flügel, A., Lund, F. E., Zhang, L. H., Potter, B. V., and Guse, A. H. (2006) Cellular effects and metabolic stability of *N*1-cyclic inosine diphosphoribose and its derivatives. *Br. J. Pharmacol.* **149,** 337–344
18. Gu, X., Yang, Z., Zhang, L., Kunerth, S., Fliegert, R., Weber, K., and Guse, A. H. (2004) Synthesis and biological evaluation of novel membrane-permeant cyclic ADP-ribose mimics: N^1-[(5″-*O*-phosphorylethoxy)methyl]-5′-*O*-phosphorylinosine 5′,5″-cyclicpyrophosphate (cIDPRE) and 8-substituted derivatives. *J. Med. Chem.* **47,** 5674–5682
19. Guse, A. H., Gu, X., Zhang, L., Weber, K., Krämer, E., Yang, Z., Jin, H., Li, Q., and Carrier, L. (2005) A minimal structural analogue of cyclic ADP-ribose: synthesis and calcium release activity in mammalian cells. *J. Biol. Chem.* **280,** 15952–15959
20. Xu, J., Yang, Z., Dammermann, W., Zhang, L., Guse, A. H., and Zhang, L. H. (2006) Synthesis and agonist activity of cyclic ADP-ribose analogues with substitution of the northern ribose by ether or alkane chains. *J. Med. Chem.* **49,** 5501–5512
21. Dong, M., Kirchberger, T., Huang, X., Yang, Z. J., Zhang, L. R., Guse, A. H., and Zhang, L. H. (2010) Trifluoromethylated cyclic-ADP-ribose mimic: synthesis of 8-trifluoromethyl-N^1-[(5″-*O*-phosphorylethoxy)methyl]-5′-*O*-phosphorylinosine-5′,5″-cyclic pyrophosphate (8-CF(3)-cIDPRE) and its calcium release activity in T cells. *Org. Biomol. Chem.* **8,** 4705–4715
22. Li, L., Siebrands, C. C., Yang, Z., Zhang, L., and Guse, A. H. (2010) Novel nucleobase-simplified cyclic ADP-ribose analogue: a concise synthesis and Ca^{2+}-mobilizing activity in T-lymphocytes. *Org. Biomol. Chem.* **8,** 1843–1848
23. Qi, N., Jung, K., Wang, M., Na, L. X., Yang, Z. J., Zhang, L. R., Guse, A. H., and Zhang, L. H. (2011) A novel membrane-permeant cADPR antagonist modified in the pyrophosphate bridge *Chem. Commun.* **47,** 9462–9464
24. Li, L. J., Lin, B. C., Yang, Z. J., Zhang, L. R., and Zhang, L. H. (2008) A concise route for the preparation of nucleobase-simplified cADPR mimics by click chemistry. *Tetrahedron Lett.* **49,** 4491–4493
25. Wu, H., Yang, Z., Zhang, L., and Zhang, L. (2010) Concise synthesis of novel acyclic analogues of cADPR with an ether chain as the northern moiety. *New J. Chem.* **34,** 956–966
26. Lagisetti, C., Urbansky, M., and Coates, R. M. (2007) The dioxanone approach to (2*S*,3*R*)-2-*C*-methylerythritol 4-phosphate and 2,4-cyclodiphosphate, and various MEP analogues. *J. Org. Chem.* **72,** 9886–9895
27. Yue, J., and Ferrell, J. E., Jr. (2006) Mechanistic studies of the mitotic activation of Mos. *Mol. Cell. Biol.* **26,** 5300–5309
28. Yue, J., Wei, W., Lam, C. M., Zhao, Y. J., Dong, M., Zhang, L. R., Zhang, L. H., and Lee, H. C. (2009) CD38/cADPR/Ca^{2+} pathway promotes cell proliferation and delays nerve growth factor-induced differentiation in PC12 cells. *J. Biol. Chem.* **284,** 29335–29342
29. Li, S., Hao, B., Lu, Y., Yu, P., Lee, H. C., and Yue, J. (2012) Intracellular alkalinization induces cytosolic Ca^{2+} increases by inhibiting sarco/endoplasmic reticulum Ca^{2+}-ATPase (SERCA). *PLoS One* **7,** e31905
30. Wong, L., Aarhus, R., Lee, H. C., and Walseth, T. F. (1999) Cyclic 3-deaza-adenosine diphosphoribose: a potent and stable analogue of cyclic ADP-ribose. *Biochim. Biophys. Acta* **1472,** 555–564
31. Furuta, T., Momotake, A., Sugimoto, M., Hatayama, M., Torigai, H., and Iwamura, M. (1996) Acyloxycoumarinylmethyl-caged cAMP, the photolabile and membrane-permeable derivative of cAMP that effectively stimulates pigment-dispersion response of melanophores. *Biochem. Biophys. Res. Commun.* **228,** 193–198
32. Higashida, H., Salmina, A. B., Olovyannikova, R. Y., Hashii, M., Yokoyama, S., Koizumi, K., Jin, D., Liu, H. X., Lopatina, O., Amina, S., Islam, M. S., Huang, J. J., and Noda, M. (2007) Cyclic ADP-ribose as a universal calcium signal molecule in the nervous system. *Neurochem. Int.* **51,** 192–199
33. Lee, H. C., Aarhus, R., Graeff, R., Gurnack, M. E., and Walseth, T. F. (1994) Cyclic ADP-ribose activation of the ryanodine receptor is mediated by calmodulin. *Nature* **370,** 307–309
34. Kolisek, M., Beck, A., Fleig, A., and Penner, R. (2005) Cyclic ADP-ribose and hydrogen peroxide synergize with ADP-ribose in the activation of TRPM2 channels. *Mol. Cell* **18,** 61–69
35. Aarhus, R., Gee, K., and Lee, H. C. (1995) Caged cyclic ADP-ribose: synthesis and use. *J. Biol. Chem.* **270,** 7745–7749
36. Liou, J., Kim, M. L., Heo, W. D., Jones, J. T., Myers, J. W., Ferrell, J. E., Jr., and Meyer, T. (2005) STIM is a Ca^{2+} sensor essential for Ca^{2+} store depletion-triggered Ca^{2+} influx. *Curr. Biol.* **15,** 1235–1241
37. Zhang, S. L., Yeromin, A. V., Zhang, X. H., Yu, Y., Safrina, O., Penna, A., Roos, J., Stauderman, K. A., and Cahalan, M. D. (2006) Genome-wide RNAi screen of Ca^{2+} influx identifies genes that regulate Ca^{2+} release-activated Ca^{2+} channel activity. *Proc. Natl. Acad. Sci. U.S.A.* **103,** 9357–9362
38. Roos, J., DiGregorio, P. J., Yeromin, A. V., Ohlsen, K., Lioudyno, M., Zhang, S., Safrina, O., Kozak, J. A., Wagner, S. L., Cahalan, M. D., Veliçelebi, G., and Stauderman, K. A. (2005) STIM1, an essential and conserved component of store-operated Ca^{2+} channel function. *J. Cell Biol.* **169,** 435–445
39. Starkus, J. G., Fleig, A., and Penner, R. (2010) The calcium-permeable nonselective cation channel TRPM2 is modulated by cellular acidification. *J. Physiol.* **588,** 1227–1240
40. Sumoza-Toledo, A., and Penner, R. (2011) TRPM2: a multifunctional ion channel for calcium signaling. *J. Physiol.* **589,** 1515–1525
41. Kirchberger, T., Moreau, C., Wagner, G. K., Fliegert, R., Siebrands, C. C., Nebel, M., Schmid, F., Harneit, A., Odoardi, F., Flügel, A., Potter, B. V., and Guse, A. H. (2009) 8-Bromo-cyclic inosine diphosphoribose: toward a selective cyclic ADP-ribose agonist. *Biochem. J.* **422,** 139–149